Supplementary information:

Nanoscale Graphene Oxide (nGO) as Artificial Receptors: Implications for Biomolecular Interactions and Sensing

Stanley S. Chou[†1], Mrinmoy De[†1]*, Jiayan Luo[1], Vincent M. Rotello[2], Jiaxing Huang[1]*, and Vinayak P. Dravid[1]*

[†]These authors contributes equally

[1]Department of Materials Science & Engineering, International Institute for Nanotechnology, Northwestern University, Evanston, Illinois 60208, United States

[2]Department of Chemistry, University of Massachusetts, Amherst, Massachusetts 01003, United States

***email: m-de@northwestern.edu, jiaxing-huang@northwestern.edu, v-dravid@northwestern.edu.**

nGO synthesis and characterization.

nGOs were synthesized according to reported procedure[1]. All materials were from Sigma Aldrich unless indicated otherwise. Briefly, 0.2 g 20 nm carbon fibers (Catalytic Materials LLC) were added to a mixture of H_2SO_4 (5ml), K_2S_2O (0.15 g) and P_2O_5 (0.15 g) at 80 ^oC. Mixture was stirred for 5 hours, cooled to room temperature, washed with DI water (200 ml) then filtered (Whatman, Grade 4), dried and transferred to a 50 ml round bottom flask. 25 ml H_2SO_4 was added and the mixture was chilled to 0 ^oC using an ice bath. $KMnO_4$ (1 g) was added to *slowly* with stirring and temperature maintained below 10 ^oC. After addition, reaction was allowed to proceed at room temperature over night. Product was transferred in to large flask and chilled to 0 ^oC with stirring. 100 ml DI water was added *slowly*, with temperature maintained below 55 °C using an ice bath. 5 ml of 30% H_2O_2 was then added *slowly*, turning solution yellow. Mixture was then *slowly* titrated with 3.4% HCL to neutralize bases. Resultant nGO mixture was collected and dialyzed against DI water for ten days using MW 7000 dialysis membranes (Sigma Aldrich). After dialysis, mixture was briefly centrifuges at 3000 rcf to remove large aggregates. Remaining nGOs were air dried, weighed and dispersed in water at 4 mg/ml concentration. Weight concentration was confirmed with lypholyzed aliquots.

Absorbance profiles of nGO were obtained by diluting successive aliquots of concentrated GO (4 mg/ml, 5 µl) in to 600 µl of 5 mM phosphate buffer (PB, pH 7.4, Figure S1a). Extinction coefficient was calculated by monitoring changes at λ = 234 nm. For the 20 nm nGO, extinction coefficient (ε_{234}) of 0.0272 ml μg^{-1} cm^{-1} was observed (Figure S1b). Considering this extinction coefficient, concentrated stock (4 mg/ml, 109 OD) was diluted to 5.9 OD (214 µg/ml) using PB for further use. Post dilution concentration (5.9 OD) was verified absorbance spectroscopy.

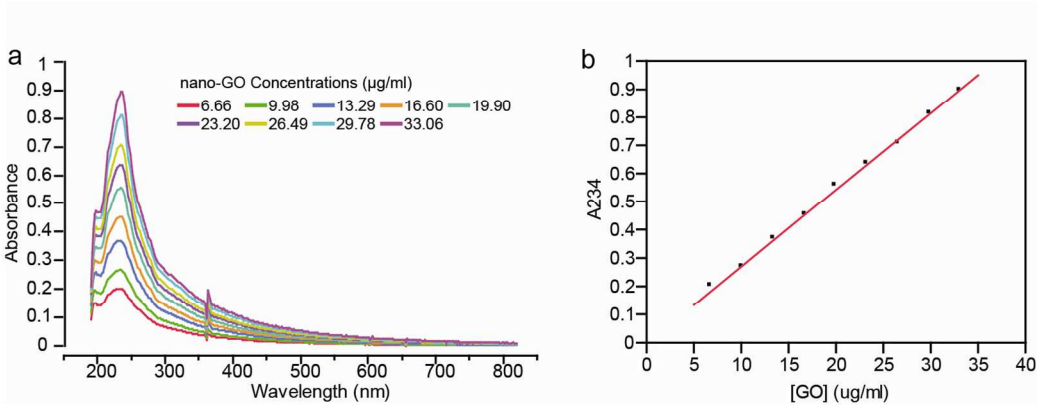

Figure S1 Calibration of nGO concentration through optical methods. **a.** Absorbance profiles of nGO in 5 mM PB, pH 7.42. **b.** Extinction coefficient of nGO was derived through linear fitting of nGO concentration (ug/ml) vs. absorbance at 234 nm. $\varepsilon_{234} = 0.0272$ ml μg^{-1} cm^{-1}

Physical characterizations of nGO were performed using DLS, TEM and AFM. DLS characterizations (diameter and zeta potential) were performed in PB using Malvern Zetasizer Nano, while TEM (Hitachi 8100) and AFM (Bruker Nanoscope III) samples were in water before desiccation. For TEM imaging, 10 ul of dilute nano GO was dropped casted onto lacey carbon grid with formvar backing (Ted Pella). Sample was allowed to dry in vacuum before TEM. Diameters of 30 specimens were measured to create the TEM size distribution. AFM samples were prepared by spin coating at 4000 RPM onto silicon substrates with 500 nm silicon dioxide. Images were acquired in tapping mode, diameters were measured by taking the FWHM of each nGO "island". In all, 24 flakes of nGO were characterized on the AFM. Resultant size distributions from all three methods can be observed in figure S2. It is important to recall that DLS measurements assume 3D spherical colloids, thus the numbers are to be taken more as the tumbling diameter of hydrated nGO in solution, rather than actual size.

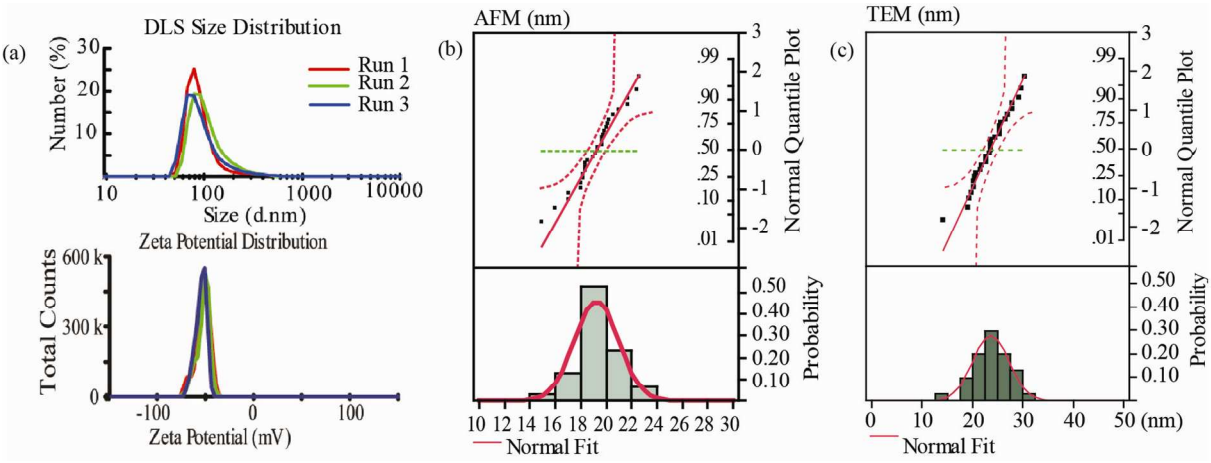

Figure S2 Size and charge characterizations of nano GO. **a**. DLS size and zeta potential distributions of nano GO. DLS measurements differ from AFM/TEM measurements because it considers colloids to be spherical, a false assumption in the case of nGOs. The resultant DLS sizes are therefore better interpreted as tumbling diameter of hydrated nGO in solution. Nonetheless, the monodispersity of nGOs is illustrated **b.** AFM size distributions of nGO in probability plot format (demonstrating Gaussian "normal" distribution) and in bar graph formal (with normal curve fitting). **c.** TEM size distributions of nGO.

Conventional-GO synthesis and characterization.

Conventional GOs were prepared using a modified Hummer's method using graphite powder (Bay carbon, SP-1). In a typical reaction, 2 g of graphite, 1 g of $NaNO_3$, and 46 mL of H_2SO_4 were stirred together in an ice bath. Next, 6 g of $KMnO_4$ was slowly added maintaining the solution temperature < 20 ^oC. Once mixed, the solution is transferred to a 35 °C water bath and stirred for about 1 h. To that green paste, 40 mL of water was added very slowly and reaction mixture was transferred to a preheated 90 ^oC water bath. The reaction mixture was stirred for 60 min. Finally, 200 mL of water was added, followed by the slow addition of 6 mL of H_2O_2 (30%). The warm solution was cooled down and washed three times with 200 ml of 10% HCL and 200 ml of water, and the filtered. The filtered cake was then dispersed in water by mechanical agitation overnight. Large aggregates were then removed by low-speed centrifugation at 500 rpm. The final product was the dialysed for two weeks with twice daily water changes.

Extinction coefficient of conventional GOs was characterized in 5 mM PB buffer. Extinction coefficient was calculated by monitoring changes at λ = 234 nm. Absorbance titration showed extinction coefficient (ε_{234}) of 0.0360 ml μg^{-1} cm^{-1} was observed (Figure S3).Size distribution were characterized by DLS and SEM (Figure S4).

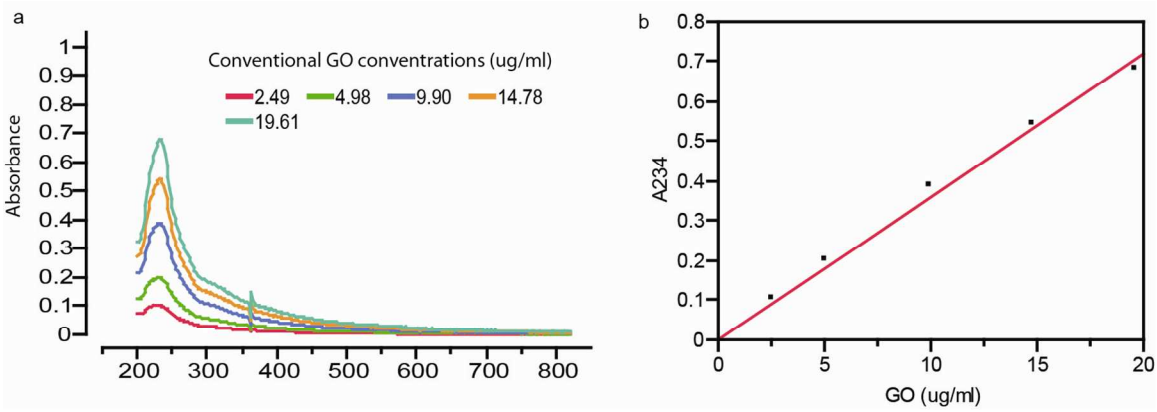

Figure S3 Calibration of conventional GO concentration through optical methods. a. Absorbance profiles of conventional GO in 5 mM PB, pH 7.42. **b.** Extinction coefficient of nGO was derived through linear fitting of nGO concentration (ug/ml) vs. absorbance at 234 nm. $\varepsilon_{234} = 0.0360$ ml μg^{-1} cm^{-1}

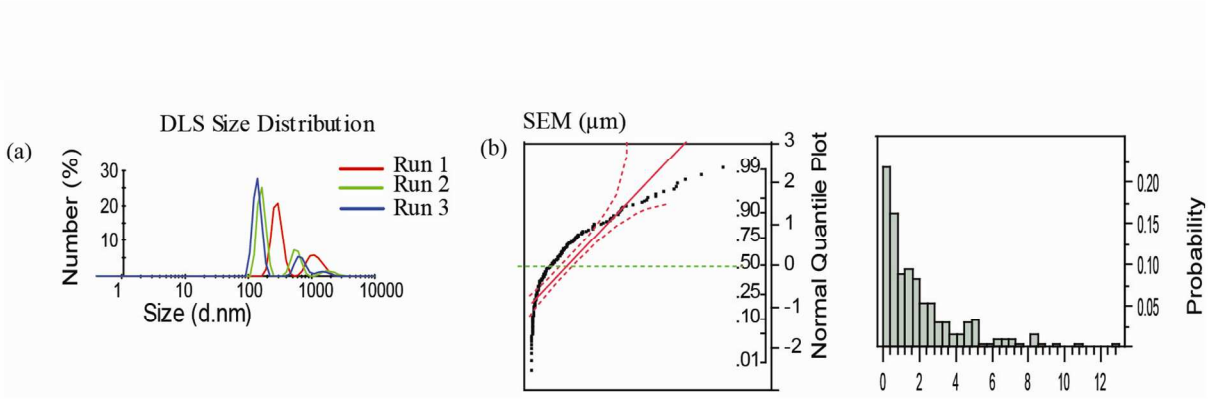

Figure S4 Size and charge characterizations of conventional GO. a. DLS size distributions of conventional GO. Due to the polydisperse nature of conventional GOs, results fluctuate greately run-run. Further DLS characterization was thus not informative.. **b.** SEM size distributions of nGO in probability plot format and in bar graph formal. The non linear nature of the probability plot demonstrates the polydisperse and non-Gaussian nature of conventionally synthesized GO.

Absorbance characterization of nGO and conventional GO:Reporter molecule complexes.

Absorbance titrations were performed to characterize changes in *fluorescent reporters* with complexation in nGO. Experiments were carried out in PB, and monitored using the HP 8452 UV/VIS spectrophotometer. To obtain appropriate absorbance profile resolution, 400 µl of PB were first spiked with concentrated fluorophores thus that $\lambda_{max} \sim 0.2$ prior to GO addition. After recording profiles of uncomplexed fluorophore, aliquots of 2 mg/ml nGO were added sequentially, with a 2 min delay in

between to allow for complexation. Absorbance profiles were recorded after each GO addition (Figure S5 and S6). In all cases, overall volume of solution changed by <4% with GO addition

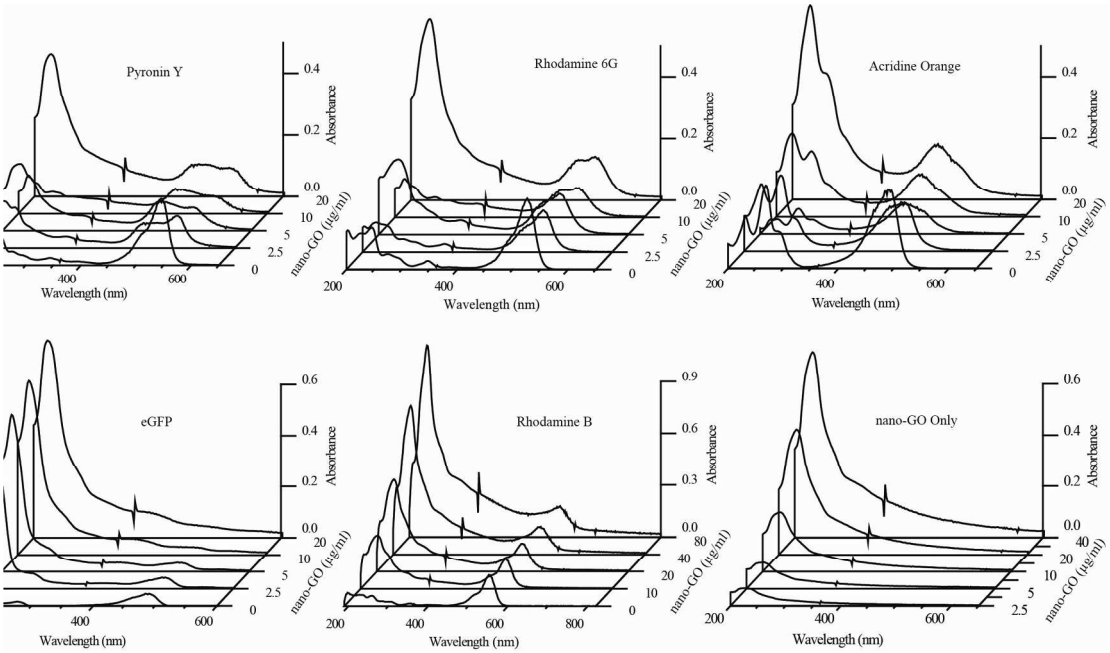

Figure S5. Absorbance profiles of various fluorophore reporters titrated with nGO.

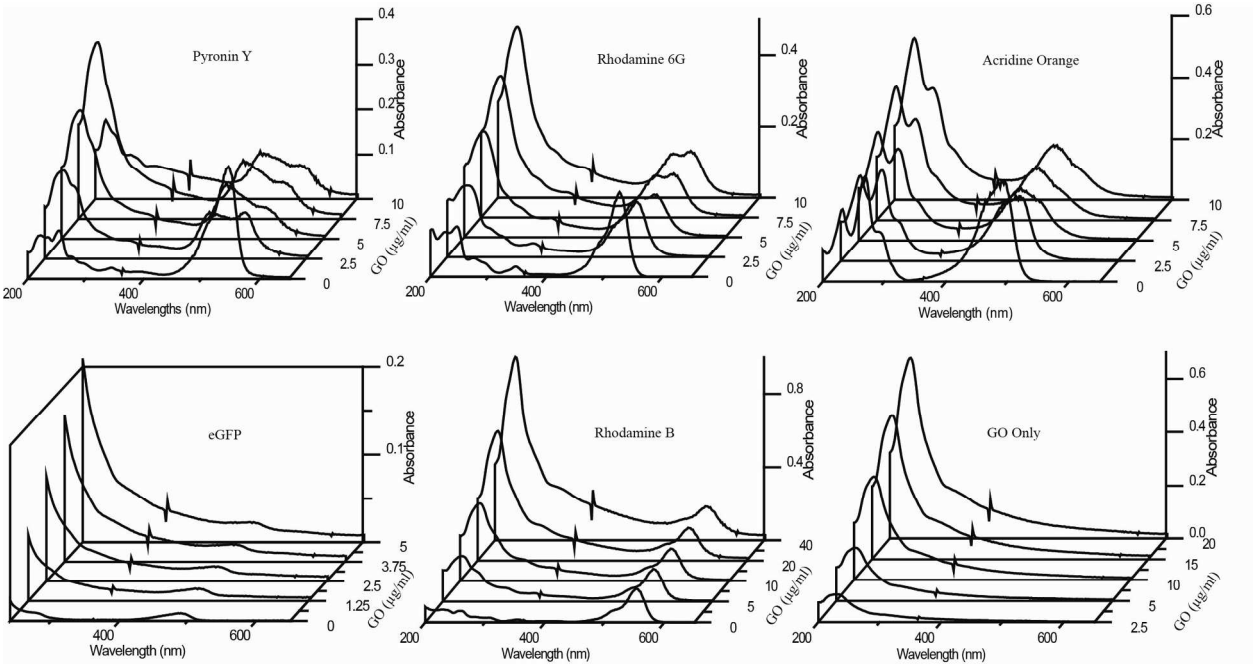

Figure S6. Absorbance profiles of various fluorophore reporters titrated with conventional GO.

Raman Characterization of conventional and nGO

Raman spectroscopy was performed to characterize changes in nGO as a consequence of complexation with reporter molecules. Samples for Raman spectroscopy were prepared by quenching the fluorescence of respective fluorophore molecules using nGO, as monitored through a UV-lamp. 5 µl of fully quenched specimens were dried on to Si substrates with 300 µm of CVD deposited SiO_2. After desiccating in vacuum for 6 hrs, samples were immediately characterized on a Nanophoton Raman-11 confocal Raman microscope (excitation wavelength 532nm)(figure S7).

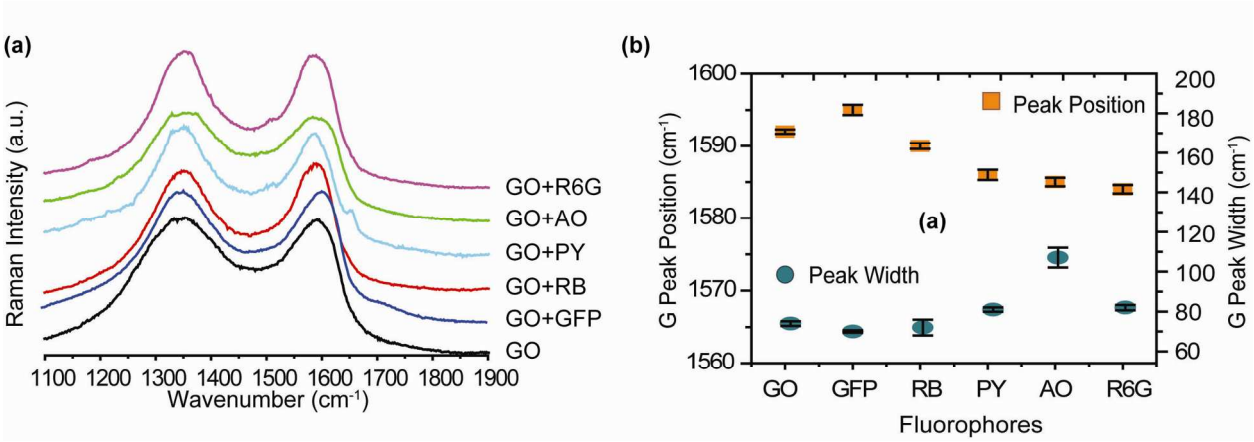

Figure S7. **(a)** Typical Raman D and G band for the conventional-GO and different fluorophore complexes. **(b)** Effect of G band frequency and width upon complexation with different fluorophore.

Fluorescent Titration of nGO and Conventional GO.

Excitation and emission wavelengths used for reporter molecules are listed below:

Reporter	$\lambda_{excitation}$ (nm)	$\lambda_{emission}$ (nm)
eGFP	475	506
Pyronin Y	535	565
Rhodamine 6G	520	548
Acridine Orange	485	528
Rhodamine B	542	574

The fluorescent titration curves were fitted by first considering the equilibrium binding constant between the fluorophores and the quenching sites on GOs.

$$K_s = \frac{[F-Q]}{[F][Q]}$$

Where [F] and [Q] are free fluorophore and quenching site concentrations respectively, and [F - Q] is the concentration of the complex. With consideration that $[F_o] = [F] + [F - Q]$, where $[F_o]$ is total fluorophore concentration, and the number of binding sites can be described by [Q] = n*[GO], the following relationship can be derived.

$$\frac{[F]}{[F_o]} = (\,1 + n * K_s\,[GO]\,)^{-1}$$

Because of this equation is similar to an inverted Stern-Volmer quenching equation, we can consider Stern-Volmer quenching constant $K_{s\text{-}v} = n*K_s$. The Stern-Volmer quenching constant therefore encompasses the quantity of fluorophores bound by individual nGOs, which can be useful for describing overall binding. All final curved were therefore fitted to the Stern-Volmer equation(figure S8 and S9). In these cases, static quenching is indicated by large $K_{S\text{-}V}$ constants.[2]

$$\frac{[F]}{[F_o]} = (\,1 + K_{S-V}\,[GO]\,)^{-1}$$

In regression analysis, the separation of variables relating to GO and fluorophore concentration allows $K_{S\text{-}V}$ to take on units dictated by [GO]. It is therefore possible to use regression to fittings by considering [GO] in g/ml or in molar concentrations. For ease of comparison, GO concentrations were converted from g/ml to molar concentrations using the density reported by Dikin et al (1.8 g/ml)[3] and the size of nano GO as measured by AFM and TEM. For nGO, a molecular weight of $6.75*10^9$ g/mol was used. Due to their polydispersity, an useful estimation of molecular weights could not be obtained for the conventional GOs.

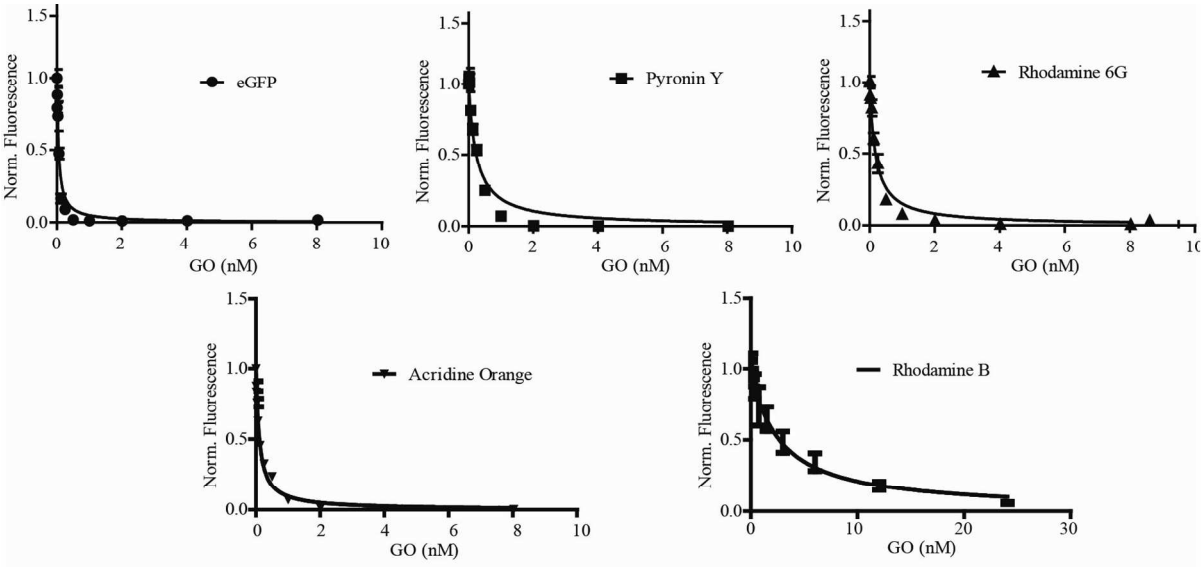

Figure S8. nGO fluorescence-quenching curves of the five fluorophores used in the initial nose array. Concentrations of fluorophores used are as followed: eGFP (9.4 nM), PY (522.9 nM), R6G (41.8 nM), AO (2.9 nM), RB (331 nM). Stern-Volmer quenching constants were determined by non-linear regression.

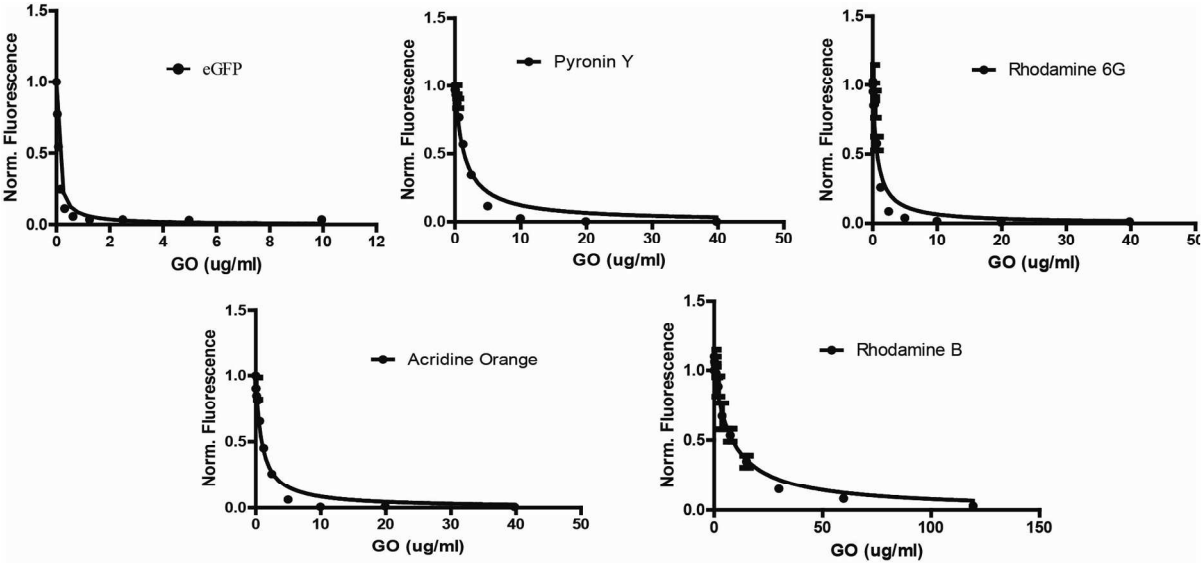

Figure S9. Conventional-GO fluorescence-quenching curves of the five fluorophores used in the initial nose array. Concentrations of fluorophores used are as followed: eGFP (9.4 nM), PY (522.9 nM), R6G (41.8 nM), AO (2.9 nM), RB (331 nM). Stern-Volmer quenching constants were determined by non-linear regression.

Table S1. The eight analyte proteins used in sensing, and their properties of interest.

Protein	MW (kDa)	pI	ε_{280} ($M^{-1}cm^{-1}$)
Bovine serum albumin (BSA)	66.3	4.8	46860
β-galactosidase (β-Gal)	540	4.6	1128600
Hemoglobin (Hem)	64.5	6.8	125000
Histone [4 4]	21.5	11	3840
Lipase (Lip)	58	5.6	54350
Lysozyme (Lys)	14.4	11	38000
Myoglobin (Mayo)	17	7.2	13940
Ribonuclease A (Rib-A)	13.7	9.4	10000

Sensing data classification

A Brief overview of Linear Discriminant Analysis (LDA)

Differential sensing utilizes many receptors that exhibit selective but nonspecific binding toward analytes. The cross-reactive nature of these receptors enables them to react to different degrees with a multitude of different analytes. They are thusly termed "differential", rather than "specific". Since these receptors are not specific for any individual analyte, their collective response in an array is unique to a particular analyte being studied. This creates a signal pattern in the array that is unique and specific for each analyte, and can be used as a "memory" or "training matrix" for identification of this analyte.[5] This approach is similar to how a mammalian nose/tongue classifies and identifies unknown odors/test.

As the array size increases, the data generated becomes gradually more complex. The accurate interpretation of this data can thus be challenging. To solve this dilemma, chemometric tools can be deployed. The most popular chemometric analysis tools have been linear discriminant analysis (LDA), principal component analysis (PCA), and hierarchical cluster analysis (HCA).[6, 7]

In LDA, the "memory" or "training matrix" is generated using "known samples." The discriminant functions are then obtained to create to maximize the separation between analyte classes while minimizing the separation within each analyte class. This approach is often called the supervised technique, since the classification of the analytes is known before the analysis. The confidence of the separation in LDA plots are checked using jack-knife analysis. The jack-knife method removes a single individual data point from the set and recreates the mathematical functions in the absence of the omitted point. That data point is then treated as a pseudo-unknown, and is re-classified in accordance with a new set of discriminant functions derived in its absence. This process is then repeated for every data point. The accuracy of the reassignment represents the classification ability of the model. Once a training matrix is complete, true unknowns can be used as inputs and classified according to the LDA plots created from the

training matrix. By calculating the Mahalanobis distance, that is, the proximity to known group centers, each unknown sample can then be identified.

Table S2. Training matrix data from 100 nM sensing experiments. Data from the nGO array and conventional GO array are shown in tandem.

	nGO					Conventional GO				
PROTEIN	**eGFP**	**PY**	**R6G**	**AO**	**RB**	**eGFP**	**PY**	**R6G**	**AO**	**RB**
β-Gal	36541.3	-4517.4	4668.9	5160.4	-144.2	2302.0	-4537.5	7255.0	3392.5	-954.5
β-Gal	43045.3	-3737.4	6992.9	2522.4	-1146.2	3849.0	-3738.5	8626.0	3697.5	6114.5
β-Gal	32189.3	-3983.4	6964.9	2409.4	-3149.2	4041.0	-4048.5	11223.0	4440.5	-51.5
β-Gal	44752.3	-3050.4	8595.9	3221.4	-871.2	3954.0	-4247.5	8958.0	4301.5	5244.5
β-Gal	42237.3	-3259.4	8536.9	2518.4	1796.8	3988.0	-4627.5	10769.0	5892.5	9202.5
BSA	5067.3	1632.6	-3197.1	-181.6	-4465.2	1322.5	-1676.5	5273.0	-363.0	-996.0
BSA	3540.3	1378.6	-1228.1	-496.6	-2685.2	1187.5	-503.5	5400.0	-90.0	661.0
BSA	3962.3	2256.6	-1489.1	-246.6	-3357.2	1130.5	-277.5	5732.0	-73.0	873.0
BSA	5238.3	3549.6	-713.1	-237.6	-2967.2	979.5	-176.5	6807.0	-79.0	207.0
BSA	5044.3	1043.6	-1909.1	-598.6	-1799.2	1005.5	-1212.5	4946.0	-254.0	605.0
Hem	20222.6	3636.8	6037.4	-1720.1	3214.5	1683.5	-2084.5	7462.0	-1116.5	4584.0
Hem	21346.6	4962.8	5546.4	-1843.1	3466.5	1776.5	-1989.5	8206.0	-1053.5	-1513.0
Hem	18338.6	4673.8	6784.4	-1779.1	2173.5	2021.5	-2163.5	5579.0	-1009.5	2946.0
Hem	18582.6	4086.8	7999.4	-1857.1	-1978.5	1933.5	-1730.5	6529.0	-1163.5	4369.0
Hem	18418.6	3167.8	7655.4	-2038.1	-919.5	1823.5	-1191.5	7486.0	-1019.5	2545.0
His	27673.3	15869.6	20397.9	3287.4	-2903.2	1565.0	2907.0	3841.5	462.5	-1127.0
His	31552.3	16073.6	27220.9	3073.4	-3446.2	1141.0	3454.0	3083.5	461.5	-4015.0
His	26198.3	15670.6	28247.9	2311.4	-2520.2	1518.0	4290.0	1671.5	577.5	-4129.0
His	29381.3	11259.6	25047.9	1049.4	-2683.2	1587.0	4592.0	3576.5	609.5	-1195.0
His	32668.3	18596.6	30154.9	2757.4	-1309.2	1702.0	4761.0	5126.5	445.5	-2380.0
Lip	1251.6	-2226.3	13037.4	-2439.1	2193.5	601.5	-2777.5	1571.5	-380.0	-1558.5
Lip	1918.6	-1022.3	13681.4	-2320.1	3880.5	613.5	-2550.5	-648.5	-363.0	-3299.5
Lip	1817.6	-1159.3	15665.4	-1973.1	5730.5	432.5	-1447.5	1016.5	-349.0	-1475.5
Lip	1491.6	-1041.3	15416.4	-1917.1	1092.5	580.5	-2773.5	1613.5	-338.0	-3276.5
Lip	2029.6	-1755.3	15101.4	-2161.1	2364.5	481.5	-2101.5	1185.5	-290.0	-4465.5
Lys	5039.1	5776.4	13037.4	1561.7	-2364.0	345.0	7702.0	16988.0	879.5	-1792.0
Lys	5611.1	3280.4	17929.4	1128.7	-2603.0	647.0	5701.0	14649.0	546.5	-3091.0
Lys	5708.1	5447.4	13681.4	1317.7	-4222.0	456.0	5200.0	15345.0	463.5	-2210.0
Lys	6059.1	6003.4	15416.4	1267.7	-2788.0	429.0	5280.0	10449.0	546.5	-2474.0
Lys	8485.1	5852.4	15101.4	1860.7	-2231.0	455.0	4432.0	16075.0	400.5	-2800.0
Myo	7637.6	920.8	11903.4	-2254.1	4197.5	1667.5	886.0	10232.0	-436.5	-342.5
Myo	6175.6	1407.8	12499.4	-1721.1	4788.5	1131.5	1206.0	11095.0	-320.5	-2613.5
Myo	9219.6	1860.8	10602.4	-1612.1	4153.5	1315.5	899.0	8456.0	-484.5	-2380.5
Myo	7108.6	1795.8	13288.4	-1770.1	4129.5	1796.5	2599.0	9336.0	-352.5	-1380.5
Myo	7903.6	1348.8	12938.4	-1825.1	2504.5	1388.5	2255.0	10302.0	-368.5	-327.5
RibA	38510.6	14011.8	1806.4	1522.9	-333.5	2055.5	5725.0	17285.0	749.5	581.5
RibA	43226.6	15482.8	121.4	1816.9	816.5	1764.5	4776.0	16086.0	738.5	-1748.5
RibA	42664.6	15721.8	1333.4	1867.9	3911.5	1798.5	5859.0	12906.0	688.5	-1516.5
RibA	45363.6	16680.8	-528.6	2421.9	3642.5	1760.5	5275.0	13378.0	884.5	-1426.5
RibA	40963.6	15940.8	219.4	1947.9	2551.5	1786.5	6713.0	18272.0	791.5	-1534.5

(a) Nano-GO array: correlation of fluorescence response to LDA scores

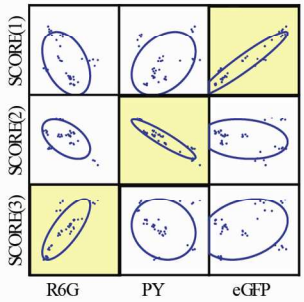

	nano-GO: R6G	nano-GO: PY	nano-GO: eGFP
Score (1)	-0.400	0.358	0.951
Score (2)	-0.498	-0.924	-0.147
Score (3)	0.770	-0.131	0.271

(b) Conventional-GO array: correlation of fluorescence response to LDA scores

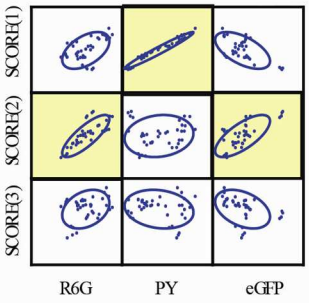

	Conventional GO: R6G	Conventional GO: PY	Conventional GO: eGFP
Score (1)	0.502	0.977	-0.580
Score (2)	0.808	0.133	0.713
Score (3)	0.309	-0.168	-0.393

(c) Nano-GO array: correlation of fluorescence response to analyte protein properties

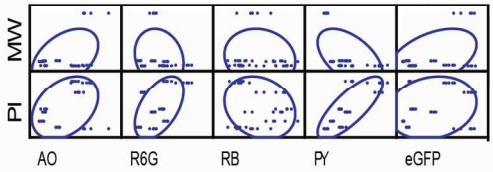

	AO	R6G	RB	PY	eGFP
MW	0.441	-0.176	-0.111	-0.535	0.460
PI	0.362	0.523	-0.209	0.784	0.162

(d) Conventional-GO array: correlation of fluorescence response to analyte protein properties

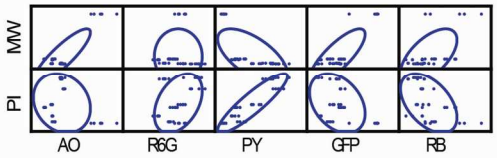

	AO	R6G	RB	PY	eGFP
MW	0.869	-0.002	-0.632	0.801	0.598
PI	-0.182	0.402	0.899	-0.351	-0.480

Figure S10. (a) Correlation of fluorescent response from the nGO array in presence of 100 nM analyte proteins, and their LDA scores. (b) Correlation of fluorescent response from the conventionalGO array in presence of 100 nM analyte proteins, and their LDA scores. (c) Correlation between the fluorescent responses of the nGO array and analyte protein properties (100 nM). Here, PY response appears strongly correlated to protein PI. For Correlations with MW, all correlations appears dominated by β-Gal's

significantly higher mass. With β-gal removed, remaining correlations are not suggestive of data interdependence. (d) Correlation between the fluorescent responses of the conventional-GO array and analyte protein properties (100 nM). Similarly to the nGO array, PY response appears to correlate strongly to PI.

Table S3. Results of 100 nM unknown sample identification using the nGO array.

Label	nGO : R6G	nGO : PY	nGO: eGFP	Identity	Prediction Accuracy (Y/N)
Unknown 01	13307.375	7039.375	6103.125	Lys	Y
Unknown 02	11368.9375	-3295.375	35171.3125	β-Gal	Y
Unknown 03	1994.375	15664.75	42379.5625	RibA	Y
Unknown 04	26513.9375	17729.625	31333.3125	His	Y
Unknown 05	15665.375	2177.375	7013.125	Lys	Y
Unknown 06	13382.375	2160.75	6730.5625	Myo	Y
Unknown 07	4353.375	3153.75	13940.5625	Hem	Y
Unknown 08	16840.375	1472.75	8063.5625	Myo	Y
Unknown 09	6817.375	6454.75	13057.5625	Hem	Y
Unknown 10	-546.0625	1539.625	7000.3125	BSA	Y
Unknown 11	17929.375	-1232.25	1252.5625	Lip	Y
Unknown 12	24817.9375	24949.625	29294.3125	His	Y
Unknown 13	8276.9375	-3639.375	24670.3125	β-Gal	Y
Unknown 14	4981.375	4025.75	25749.5625	Hem	Y
Unknown 15	20083.9375	20281.625	35987.3125	His	Y
Unknown 16	7030.375	15895.75	41790.5625	RibA	Y
Unknown 17	12093.375	-2123.25	2359.5625	Lip	Y
Unknown 18	3789.9375	-4763.375	41451.3125	β-Gal	Y
Unknown 19	-706.625	15785.75	42699.5625	RibA	Y
Unknown 20	992.9375	3704.625	6733.3125	BSA	Y
Unknown 21	13307.375	-2093.25	1819.5625	Lip	Y
Unknown 22	13167.375	1523.75	7290.5625	Myo	Y
Unknown 23	12093.375	6548.375	8271.125	Lys	Y
Unknown 24	333.9375	3027.625	8071.3125	BSA	Y

Table S4. Results of 100 nM unknown sample identification using the conventional GO array.

Label	Conventional GO: R6G	Conventional GO: PY	Conventional GO: eGFP	Identity	Prediction Accuracy (Y/N)
Unknown 01	8444.5	370.5	980.5	BSA	N
Unknown 02	28218	4651	1617	His	N
Unknown 03	12550.5	-914.5	1850.5	Hem	Y
Unknown 04	9175.5	-3777.5	3168	β-Gal	Y
Unknown 05	21261.5	6577	1726.5	RibA	Y
Unknown 06	3063.5	-1882.5	406.5	Lip	Y
Unknown 07	8895.5	2604	1496.5	Myo	Y
Unknown 08	11237.5	1902	1037.5	Myo	Y
Unknown 09	20442	4110	428	Lys	Y
Unknown 10	12601.5	-3626.5	2921	b-Gal	Y
Unknown 11	4603.5	-623.5	193.5	Lip	N
Unknown 12	20242	4475	401	Lys	Y
Unknown 13	7556.5	-1022.5	1628.5	Hem	Y
Unknown 14	10333.5	2364	1323.5	Mayo	Y
Unknown 15	31767	5271	1416	His	N
Unknown 16	26616	4422	1569	His	N
Unknown 17	22425	3376	529	Lys	Y
Unknown 18	8893.5	-1297.5	1769.5	Hem	Y
Unknown 19	5811.5	-815.5	1087.5	BSA	N
Unknown 20	18654.5	6675	1615.5	RibA	Y
Unknown 21	14532.5	-2578.5	3077	β-Gal	Y
Unknown 22	5594.5	-1645.5	246.5	Lip	Y
Unknown 23	9265.5	1806.5	1243.5	BSA	N
Unknown 24	19479.5	6558	1861.5	RibA	Y

T**able S5.** Training matrix data from 10 nM sensing experiments.

	nGO			Conventional GO		
PROTEIN	**eGFP**	**PY**	**R6G**	**eGFP**	**PY**	**R6G**
β-Gal	6042.3	-4909.4	2072.9	720.0	-3672.0	10207.0
β-Gal	5382.3	-2735.4	3728.9	788.0	-3462.0	8336.0
β-Gal	6712.3	-4448.4	3446.9	603.0	-3223.0	8384.0
β-Gal	6179.3	-4522.4	6275.9	516.0	-3506.0	7764.0
β-Gal	6564.3	-3801.4	5753.9	555.0	-2622.0	7082.0
BSA	-4.7	-2479.4	1867.9	39.0	-1263.0	1907.0
BSA	-6.7	-2151.4	-1060.1	-13.0	-704.0	3176.0
BSA	16.3	-1986.4	-1662.1	25.0	-975.0	3580.0
BSA	19.3	-2167.4	1326.9	-11.0	-677.0	820.0
BSA	-93.7	-2393.4	2475.9	-16.0	-581.0	707.0
Hem	3026.6	13.8	4424.4	587.0	1320.0	10530.0
Hem	3170.6	898.8	1456.4	462.0	506.0	7998.0
Hem	2095.6	1957.8	2796.4	498.0	1795.0	6896.0
Hem	3630.6	1752.8	2244.4	606.0	544.0	4640.0
Hem	2641.6	1470.8	2877.4	433.0	874.0	5252.0
His	1317.3	4914.6	6583.9	407.0	301.0	2731.0
His	1724.3	5490.6	8707.9	248.0	517.0	3126.0
His	1548.3	5119.6	8722.9	236.0	796.0	1026.0
His	1279.3	5276.6	6438.9	256.0	636.0	3673.0
His	886.3	5690.6	7182.9	421.0	1047.0	1807.0
Lip	325.6	-3159.3	13553.4	1.0	1463.0	1090.0
Lip	249.6	-1844.3	8876.4	69.0	-1033.0	1563.0
Lip	345.6	-1851.3	11157.4	21.0	-755.0	-201.0
Lip	308.6	-2020.3	11029.4	-3.0	-783.0	200.0
Lip	347.6	-2017.3	9092.4	-9.0	-334.0	-728.0
Lys	1172.1	1459.4	13553.4	-61.0	846.0	4079.0
Lys	2683.1	3043.4	9092.4	-43.0	1166.0	5479.0
Lys	948.1	1109.4	11157.4	-59.0	584.0	4747.0
Lys	1251.1	2098.4	10212.4	-60.0	836.0	4760.0
Lys	1463.1	2144.4	11029.4	69.0	1153.0	3788.0
Myo	1113.6	1137.8	3053.4	347.0	3577.0	1470.0
Myo	1054.6	739.8	2009.4	176.0	921.0	2793.0
Myo	1029.6	1598.8	1846.4	145.0	725.0	1189.0
Myo	1039.6	959.8	2635.4	179.0	700.0	567.0
Myo	1383.6	732.8	3145.4	36.0	556.0	3840.0
RibA	9538.6	2996.8	5780.4	578.0	-545.0	4139.0
RibA	11116.6	2828.8	6700.4	576.0	-29.0	5519.0
RibA	10372.6	4269.8	2770.4	429.0	-44.0	3896.0
RibA	9091.6	3628.8	3634.4	428.0	-186.0	4164.0
RibA	9873.6	4195.8	-541.6	565.0	275.0	6351.0

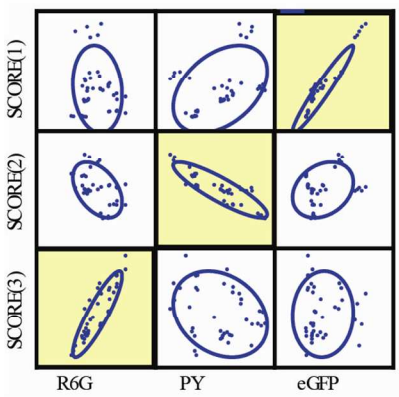

	nano-GO: R6G	nano-GO: PY	nano-GO: eGFP
SCORE(1)	-0.131	0.408	0.961
SCORE(2)	-0.441	-0.878	0.273
SCORE(3)	0.888	-0.252	0.0414

Figure S11. Protein discrimination at 10 nM using only three dimensions (R6G, PY and eGFP) demonstrated comparable results to separation using five dimensions. This further validated the redundancy of the discarded dimensions, RB and AO.

Table S6. Unknown identification at 10 nM using nGO array.

Label	nGO: R6G	nGO: PY	nGO: eGFP	Identity	Prediction Accuracy (Y/N)
Unknown 01	2635.9375	-1868.375	8.3125	BSA	Y
Unknown 02	8876.375	1088.375	1126.125	Lys	Y
Unknown 03	7330.375	1170.75	2075.5625	Hem	Y
Unknown 04	993.375	681.75	1092.5625	Myo	Y
Unknown 05	7836.9375	7758.625	1294.3125	His	Y
Unknown 06	1447.375	66.75	1130.5625	Myo	Y
Unknown 07	4173.9375	10038.625	1158.3125	His	Y
Unknown 08	4116.375	1984.75	2571.5625	Hem	Y
Unknown 09	13908.375	4174.75	12467.5625	RibA	Y
Unknown 10	9092.375	-2017.25	347.5625	Lip	Y
Unknown 11	3262.375	2579.75	3447.5625	Hem	Y
Unknown 12	2637.9375	-3960.375	5111.3125	β-Gal	Y
Unknown 13	5883.9375	-2911.375	3476.3125	β-Gal	Y
Unknown 14	9092.375	3043.375	2683.125	Lys	Y
Unknown 15	7741.9375	5229.625	2194.3125	His	Y
Unknown 16	10212.375	-781.25	481.5625	Lip	Y
Unknown 17	11236.375	4507.75	9742.5625	RibA	Y
Unknown 18	17853.375	2489.375	615.125	Lys	Y
Unknown 19	5358.375	-3121.25	203.5625	Lip	N
Unknown 20	4648.9375	-3630.375	4371.3125	β-Gal	Y
Unknown 21	3946.375	4425.75	8247.5625	RibA	Y

Unknown 22	-2146.0625	-1542.375	137.3125	BSA	Y
Unknown 23	1281.375	-769.25	1039.5625	Myo	N
Unknown 24	-1217.0625	-554.375	-14.6875	BSA	Y

References:

1. Luo, J.; Cote, L. J.; Tung, V. C.; Tan, A. T. L.; Goins, P. E.; Wu, J.; Huang, J., Graphene Oxide Nanocolloids. *J. Am. Chem. Soc.* **2010,** *132* (50), 17667-17669.
2. Lakowicz, J. R., *Principles of Fluorescence Spectroscopy*. 3rd ed.; Springer: New York, NY, 2006; p 305.
3. Dikin, D. A.; Stankovich, S.; Zimney, E. J.; Piner, R. D.; Dommett, G. H. B.; Evmenenko, G.; Nguyen, S. T.; Ruoff, R. S., Preparation and characterization of graphene oxide paper. *Nature* **2007,** *448* (7152), 457-460.
4. Sahoo, D.; Seita, J.; Bhattacharya, D.; Inlay, M. A.; Weissman, I. L.; Plevritis, S. K.; Dill, D. L., MiDReG: A method of mining developmentally regulated genes using Boolean implications. *Proc. Natl. Acad. Sci. USA* **2010,** *107* (13), 5732-5737.
5. Adams, M. M.; Joyce, L. A.; Anslyn, E. V., Uses of Differential Sensing and Arrays in Chemical Analysis. In *Supramolecular Chemistry: From Molecules to Nanomaterials*, Steed, J. W.; Gale, P. A., Eds. Wiley: 2012; Vol. 2, pp 709-730.
6. Joliffe, I. T., *Principal Component Analysis*. 2nd ed.; Springer-Verlag: New York, 2002.
7. Johnson, R. A.; Winchern, D. W., *Applied Multivariate Statistical Analysis*. Prentice-Hall: New Jersey, 1982.